



First validation experiments of the prototype solid state RF system for IFMIF-DONES

Cristina de la Morena ^{a,*}, David Regidor ^{a,b}, Daniel Iriarte ^c, Francisco Sierra ^c, Eduardo Ugarte ^c, Saša Dragaš ^d, Paolo Marini ^d, Joaquin Molla ^a, Angel Ibarra ^a

^a Laboratorio Nacional de Fusión (LNF), Centro de Investigaciones Energéticas, Medioambientales y Tecnológicas (CIEMAT), Madrid, Spain

^b Universidad Nacional de Educación a Distancia (UNED), Madrid, Spain

^c Broad Telecom SA (BTESA), Leganés, Spain

^d RYMSA Sener Aeroespacial, Arganda del Rey, Spain



ARTICLE INFO

Keywords:

IFMIF-DONES
Radiofrequency power systems
Resonant cavity combiner
Solid-state amplifiers

ABSTRACT

Following the current tendency towards solid-state (SS) amplification technology, the IFMIF-DONES (International Fusion Materials Irradiation Facility - DEMO-oriented Neutron Source) Radiofrequency (RF) Power System will be fully based on SS technology. A challenging issue in high power SS amplifiers is focused on the search of an efficient combination technique for a very large number of power signals. A promising RF power combination technique has been proposed for IFMIF-DONES: a resonant cavity combiner. The crucial characteristic of this combining technology is that the high power combination is achieved in just one step, by means of coupling the outputs of a large number of active devices into a resonant circuit. This improves the efficiency compared with traditional corporate topologies, which is a key aspect for SS amplifiers. In addition, it results in a very compact design, although its circular shape may complicate the design of other SSPA components, which are more standardized for rectangular cubicles or rack solutions. In order to demonstrate the feasibility of this combination technology for the IFMIF-DONES RF Power System, a prototype cavity combiner has been designed and fabricated. It has been validated at small-signal and at medium-high power levels: up to 24 kW in continuous wave (CW) and 100 kW in pulsed mode (duty cycle DC = 4%). The design of this prototype combiner and the results of the first validation experiments are presented in this paper.

1. Introduction

Vacuum-tube technology remains the main candidate for very high power levels or for high frequencies. Nevertheless, for frequencies typically below L band and mid-range power levels (from few kW to hundreds of kW) [1], SS technology is a strong alternative with important benefits: reliability, high modularity with associated redundancy and flexibility, availability, absence of high voltage, lower phase noise, longer lifetime, hot-swapping during operation, simpler and faster start-up procedure, and easier maintenance [1–3].

The pioneers in replacing vacuum tubes by SS amplifiers were Ti Ruan and his team at LURE-Orsay in the 1990s [4]. This research was followed by SOLEIL synchrotron in the 2000s (1 × 35 kW, 4 × 180 kW SS amplifiers at 352 MHz) [5], which has demonstrated a successful experience of more than ten years [6]. The maturity of the SS technology and the cost reduction in the last years have motivated that many large

scientific facilities have selected SS for upgrading or developing their RF power systems [6,7]: European Synchrotron Radiation Facility (ESRF, France, 150 kW at 352 MHz), Laboratório Nacional de Luz Síncrotron (LNLS, Brazil, 50 kW at 476 MHz), X-ray source ThomX (France, 50 kW at 500 MHz), Diamond Light Source (UK, 80 kW at 500 MHz), BESSY II (Germany, 1 × 40 kW and 4 × 80 kW at 500 MHz), ALBA (Spain, 50 kW at 500 MHz), MYRRHA (Belgium, 192 kW at 176 MHz), MAX IV (Sweden, 60 kW at 100 MHz), Fermilab (USA, 75 kW at 162 MHz and 200 kW at 650 MHz), SPRING-8 (Japan, 110 kW at 508.7 MHz), Canadian Light Source (CLS, Canada, 100 kW at 500 MHz), CERN Super Proton Synchrotron (SPS, Switzerland, 16 × 144 kW = 2 MW peak at 200 MHz), etc. On the same trend line and from the experience of the SS power amplifiers (SSPA) developed for LIPAc (Linear IFMIF Prototype Accelerator) project [8,9], the IFMIF-DONES RF Power System will be fully based on SS technology [10–12]. It will be composed of 56 RF stations, providing a total of 7.4 MW of RF power at 175 MHz in CW. The most

* Corresponding author.

E-mail address: cristina.delamorena@ciemat.es (C. de la Morena).

power-demanding RF stations will provide up to 200 kW in CW.

In such high power SS amplifiers, the RF power combination of a large number of transistors outputs is required, which adds complexity and degrades efficiency. The search of an efficient combination stage is indeed a crucial and challenging issue in SS power amplifiers (SSPAs). The typical combination topology consists of corporate configurations, also called tree power combining, where several combination stages are used. The larger the number of combination stages, the higher the efficiency degradation. A promising combination technology based on resonant cavity allows a high power single-step combination, with a reduction in the losses and the space with respect to corporate-combining schemes. The first cavity combiner with a large number of inputs (132) was proposed by ESRF under research program EU/FP7/ESFRI/CRISP [13], which was validated in a 85 kW 352 MHz SSPA prototype [3,7]. CERN, who was involved in the project as partner, has continued this work in the SPS 200 MHz SSPAs [14]. Other SSPA projects following ESRF cavity combiner approach are currently under study or development: Advanced Photon Source (APS) at Argonne National Laboratory (352 MHz) [15], SPRING-8 (508.7 MHz) [16], PIP-II at Fermilab (650 MHz) [17], and IFMIF-DONES (175 MHz) [10–12]. ESRF reached 85 kW in CW operation without thermal problems, as in their design the 132 RF power modules are mounted on 22 water cooled wings, which constitute the side walls of the cylindrical cavity combiner. CERN SSPAs work in pulsed mode and no technical details have been published due to the non-disclosure agreement with Thales. APS, SPRING-8, PIP-II, and IFMIF-DONES cavity combiner prototypes do not include cooling system, and the reported experiments have revealed efficiency degradation due to the temperature increment, pointing out to the need of water cooling and cavity tuning strategy for CW systems. APS has validated its cavity combiner prototype at 6 kW CW during 6 h, SPRING-8 has reached 1.88 kW CW, and PIP-II 2.8 kW CW. In [12] the first cavity combiner prototype for IFMIF-DONES was validated in an experimental campaign up to 5 kW in CW and at 100 kW in pulsed mode (DC = 4%). However, a thorough thermal characterization should be useful to determine the cavity frequency detuning and the efficiency degradation, which requires increasing the power of the experiments.

As the high-power validation strategy followed by most of the authors is based on the cavity combiner and SSPA modules integration, it makes difficult to independently characterize the cavity combiner, and the RF power increment raises the complexity of the experiment (balance among amplifiers is required). In this paper a different experimental validation strategy is presented, which allows an independent characterization of the cavity combiner performance. The experimental validation of the cavity combiner prototype used in [12] has been extended up to 24 kW in CW during 3 h. The prototype was modified with that purpose, thanks to its modular design, which makes possible to modify the input-ports configuration without fabricating a new prototype. Beyond the analysis of the RF fields and the achieved combination efficiency, the experiment has allowed analyzing the thermal behavior and the resonant frequency and efficiency variation.

2. Prototype resonant cavity combiner

2.1. Theory of resonant cavity combiners

Resonant cavity combiners are based on cylindrical or pillbox cavities operating in the Transverse Magnetic mode TM_{010} [3,12,18]. The electrical field has a longitudinal distribution, whose maximum is in the center of the cavity, and the magnetic field is maximal in the cavity walls, as shown in Fig. 1. Current, which is the responsible of the ohmic losses, is distributed on the walls surface. The theory of this combination technique is presented in detail in [12], together with a failure behavior analysis. Note that its behavior can be modeled as a resonant non-isolated N-way combiner, being N the number of input ports.

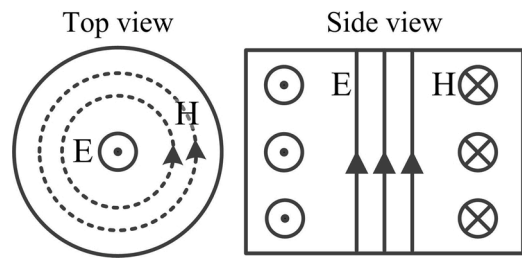


Fig. 1. Field distribution in a pill-box cavity in TM_{010} mode.

2.2. Design and implementation

A first cavity combiner was designed and fabricated, as a prototype of the SS RF System that could be used for the IFMIF-DONES accelerator [10,11]. The detailed design, the implementation, and the preliminary experimental validation have been published in [12]. Like in the ESRF approach, the fabricated cavity combiner is not a single solid structure. It is modelled as a quasy-cylindrical forty-sided prism, composed of forty plates whose internal walls are flat. The plates can incorporate input current loops or they can be blind plates. Therefore, blind plates can be removed from the structure and substituted by plates with loops, changing the number of inputs using the same combiner. This modular design is more susceptible to RF leakages through the joints of the walls, but it is very advantageous because it opens the possibility of having a port-reconfigurable cavity combiner.

The ESRF combiner was firstly configured with 18 input modules on three wings and 19 blind plates for intermediate tests. It was later upgraded to 132 input modules to reach 85 kW CW by simply readjusting the output coupling in order to re-establish a perfect matching. In [12] the IFMIF-DONES prototype cavity combiner was configured with twenty inputs, five inputs per column with N-type RF connectors. In this case, the loop design was based on circular loops fabricated by shaping copper round rods with a tool in a manual process. A new version of the cavity combiner prototype is presented, with four inputs per column and a total of sixteen 7/8"-type inputs, which could be upgraded to 160 inputs. The photograph of the sixteen-input cavity combiner prototype is shown in Fig. 2.

This sixteen-input version incorporates a new loop design, shown in Fig. 3, which provides the following advantages:



Fig. 2. Sixteen-input cavity combiner prototype.



Fig. 3. New input loop design: four inputs per column.

- Higher power-handling capability.
- More robust structure (machined monoblock).
- No weldings: the loops are screwed to the cavity.
- Lower temperature.
- Easier and cheaper to manufacture.
- Faster (dis)connection of the amplifiers.

3. Experimental validation

3.1. Small signal characterization

The Rohde&Schwarz ZNB4 Vector Network Analyzer (VNA) has been used for the scattering parameters measurement. The VNA has been connected to the R&S ZN-Z84 Switch Matrix, which allows extending the number of test ports up to 24. An EIA 6 1/8" to 3 1/8" transition followed by a 3 1/8" to N transition are placed at the cavity combiner output, in order to connect to the ZN-Z84 Switch Matrix. The measured amplitude scattering parameters for one of the upper ports are presented in Fig. 4. At the nominal 175 MHz frequency, the output return loss is -27.1 dB, and the input return loss is -0.48 dB (ideal value $20\log_{10}(15/16) = -0.56$ dB). In spite of the high input return loss value, note that when all inputs are symmetrically excited there is no reflected power at the input ports, because the reflected signal coming from the own excitation is cancelled with the signals coupled from the other excited input ports (isolation). Isolation parameters are below -25.2 dB, being the theoretical value $20\log_{10}(1/16) = -24.08$ dB. The measured amplitude transmission parameters are close to the theoretical value of $20\log_{10}(1/\sqrt{16}) = -12$ dB, being in the range of -12.6 and -12.26 dB. These imbalances among ports will entail a reduction in the combiner efficiency, which could be solved by reducing gradually the penetration of the loops from the bottom to the top of the column, in order to increase the coupling of the upper loops, as they present worse

coupling. In the prototype all loops are equal in order to facilitate the loops manufacturing process and to optimize repeatability. Table 1 compiles the measured main parameters of both prototype versions: 20 and 16 inputs. Note that there has not been alteration in the cavity combiner electromagnetic performance, while the mechanical characteristics and the power handling capability of input loops have been improved with the new loop design.

3.2. Power tests results

The cavity combiner is a symmetrical device, hence it is possible to perform the validation indistinctly working as a combiner or as a divider. In case of divider-mode operation, the validation experiment is more practical and easy to implement, since only one RF source is required as input (instead of multiple RF sources in combiner-mode operation). The test bench is shown in Fig. 5. The four outputs of one column will be combined by means of a 4:1 primary combiner, custom-made by BTESA. Next, the outputs of these four 4:1 combiners will be combined once again in a final 4:1 power combiner (RYMSA Power Splitter DT13 series), which is connected to a high power load for the RF power dissipation. The maximum power for this experiment is limited by the final 4:1 combiner power handling capability: 6 kW per input in CW. This entails a maximum power of 24 kW in CW at the cavity combiner input.

The RF source that has been used for the experiment is the prototype RF chain manufactured for the RF System of the LIPAC (Linear IFMIF Prototype Accelerator) Project [8,19]. It is a 175 MHz 200 kW RF chain composed of three amplification stages: a first solid-state pre-driver, and two tetrodes as driver (Thales TH561) and final amplifiers (Thales TH781). The RF chain is protected against reflected power by means of a circulator. The 175 MHz signal is generated by the Low Level RF System, which is the same system developed by CIEMAT and Seven Solutions for the LIPAC Project [20].

The photograph of the experiment is included in Fig. 6. The cavity combiner was progressively excited in CW from 0 kW to 24 kW, and then it was kept to 24 kW during three hours, when thermal stabilization was reached. Meanwhile, the following measurements were taken:

- Temperature measurements: they were tested by thermocouples placed on the cavity external wall at the points called T1 (row 1, upper loop), T2 (row 2, second loop), and T3 (blind column, without loops), shown in Fig. 6.
- RF signals measurements: they were tested at the points indicated in Fig. 6. The input (P_{in}) and output (P_{out}) powers were measured using the KEYSIGHT N1914A power meter and N8482A power sensor. The input return loss, i.e. the relation $Fw-Rv$ (dB), was measured by the LLRF system.
- RF leakage measurements: the RF leakage through the cavity walls to the outside was measured using an electromagnetic field meter.

The time evolution of P_{in} , P_{out} , temperatures, and input return loss ($Fw-Rv$) are presented in Fig. 7. The difference between the measured P_{in} and P_{out} values is presented in Fig. 8 as a function of the temperature measured at T1. The next conclusions can be extracted from the experiment:

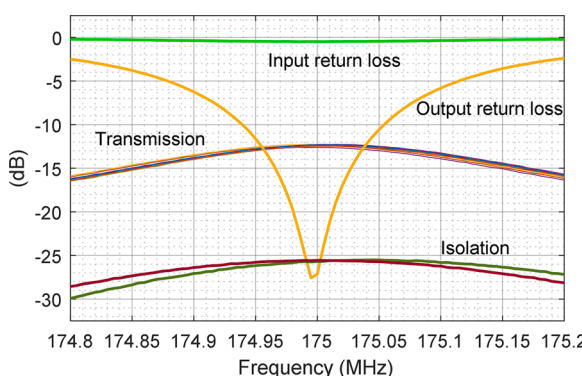


Fig. 4. Measured amplitude scattering parameters.

Table 1
Measured main parameters of the two cavity combiner versions.

Parameter	First version (20 inputs)	Second version (16 inputs)
Resonant freq. f_0 (MHz)	174.998	175.000
Bandwidth BW (kHz)	331.95	340.0
Quality factor Q	527.167	514.6
Losses at f_0 (dB)	0.394	0.378
Efficiency (%)	91.32	91.64

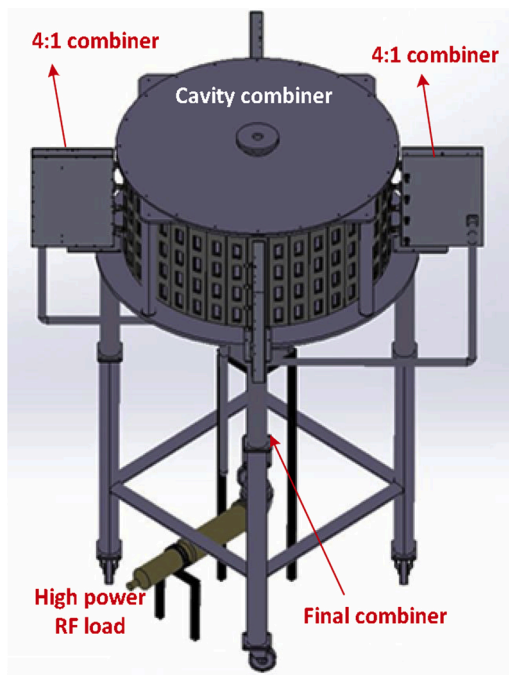


Fig. 5. Test bench for the power validation experiment.

- Temperature: it reaches stabilization at 52 °C in T1 and T2, and at 47 °C in T3. T1 and T2 have 5 °C more than T3 because they are measured close to the loops, while T3 is measured in a blind plate.
- Frequency tuning: the cavity resonant frequency varies with the temperature, as it can be seen through the variation of the return loss, represented as F_{w-Rv} (dB) in Fig. 7. Matching is maximum at 35°, with a value of 32 dB. For higher temperatures, it starts to decrease, although it never drops below 20 dB for all temperatures.
- RF leakage: significant values of electric field are measured in the vicinity of the cavity combiner: 99 V/m (Max. Avg. value@24 kW). This entails additional losses that reduce the combination efficiency, hence a better shielding must be achieved.
- Combination losses/efficiency: the difference between P_{in} and P_{out} at 175 MHz, shown in Fig. 8, represents the losses produced by all the different stages: 16-inputs cavity divider, primary 4:1 combiners, and final 4:1 combiner. The measured losses (combination + ohmic losses) of the primary 4:1 combiners are compiled in Table 2. The

insertion loss of the final combiner is < 0.05 dB, and its power unbalance between ports is ± 0.2 dB (values from data sheet). In addition, calibration errors in the RF test points must not be disregarded, as the RF signals are measured through bidirectional couplers with high attenuation (60–65 dB). As for the laboratory instrumentation, the measurement uncertainty of N8482A power sensor is ± 0.35 %. Consequently, the estimated losses due to the cavity combiner might be around 0.2–0.4 dB lower than the measured $P_{in} - P_{out}$ values of Fig. 7. This results in a cavity combiner efficiency between 91–95 %

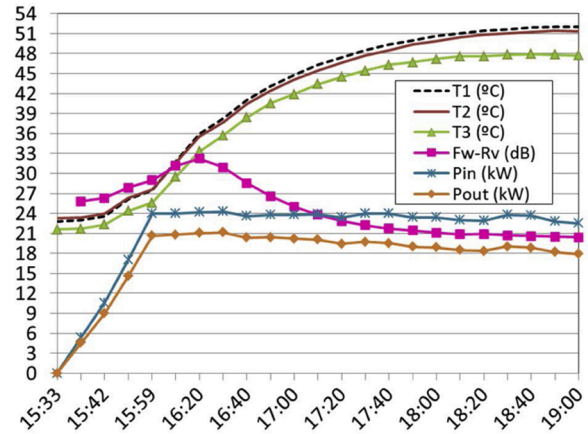


Fig. 7. Test results of power validation experiment: 24 kW CW during 3 h.

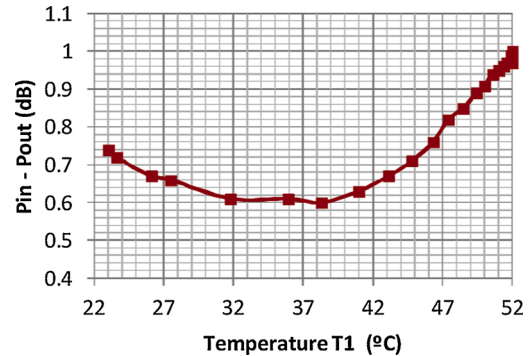


Fig. 8. Total losses measured at 175 MHz versus temperature.

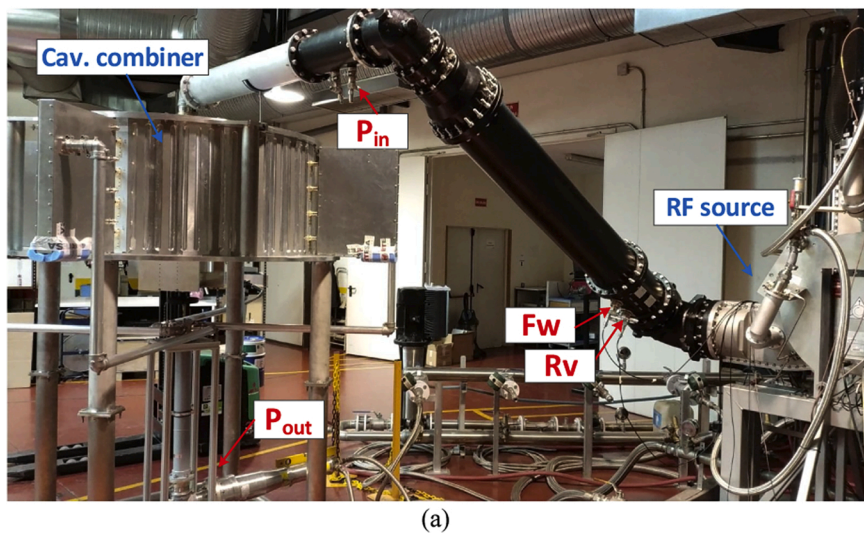


Fig. 6. Power experiment and measurement points of (a) RF signals and (b) temperatures.

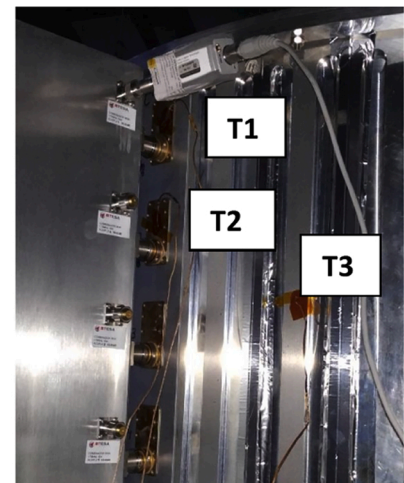


Table 2

Measured losses of the primary 4:1 combiners.

Component	Losses @ 175 MHz (dB)
4:1 combiner #1	0.057
4:1 combiner #2	0.040
4:1 combiner #3	0.078
4:1 combiner #4	0.044

at the best condition point (35 °C). The evolution of losses with temperature obviously follows the same tendency of return loss: the best tuning point, located at 35 °C, is the best point for combination loss/efficiency. From ambient temperature to 35 °C losses decrease, while they increase as the temperature rises from 35 °C. Total losses degrade 0.4 dB from 35 °C to 52 °C, which in terms of efficiency is 8 points in percentage. It seems clear that water cooling and frequency detuning compensation is needed if high combination efficiency is wanted to be maintained in CW and high power.

4. Conclusions and future work

A single-step multi-port and efficient combination technology has been presented in this paper as a candidate for the SS RF System of IFMIF-DONES. It has been validated at 24 kW in CW and at 100 kW in pulsed mode (DC = 4%), achieving very promising results as for efficiency. Furthermore, it is worth to mention that there is still margin for efficiency improvement from this first prototype: plating the internal cavity walls to decrease cavity losses, improving imbalances among ports and the shielding to avoid RF leakage through the walls, including an automatic tuning system, etc. The CW high power experiments have allowed the analysis of the cavity combiner thermal behavior with respect to resonant frequency deviation and consequent efficiency degradation. If high combination efficiency is wanted to be maintained, the conclusions point out the need of water-cooling and detuning compensation in the cavity combiner for CW and high power SSPAs.

Current and future work is focused on the design and development of an industrial water-cooled 160-input cavity combiner, which incorporates an automatic tuning system. The objective is to validate it at high RF power, 200 kW in CW, in order to finally demonstrate the feasibility of this combination technology and its applicability to the RF Power System of IFMIF-DONES, as well as other accelerators or scientific facilities. Furthermore, the design and development of the SS high power amplifiers for the RF System of IFMIF-DONES are within the current and future activities, with special focus on the improvement of the efficiency and availability.

Declaration of Competing Interest

The authors declare that they have no known competing financial interests or personal relationships that could have appeared to influence the work reported in this paper.

Acknowledgments

This work has been carried out within the framework of the

EUROfusion Consortium and has received funding from the Euratom research and training programme 2014–2018 and 2019–2020 under grant agreement No.633053. The views and opinions expressed herein do not necessarily reflect those of the European Commission.

This work has been received funding from the Spanish Centre for the Development of Industrial Technology (CDTI) under CIEN 2016 program IDI-20160850 for the development of the ACTECA project.

References

- [1] F. Gerigk, Status and future strategy for advanced high power microwave sources for accelerators, in: Proc. of IPAC 2018, Vancouver, BC Canada, 2018, pp. 12–17, <https://doi.org/10.18429/JACoW-IPAC2018-MOYGB1>.
- [2] M. Di Giacomo, Solid state RF amplifiers for accelerator applications, in: Particle Accel. Conf. (PAC09), Vancouver, Canada, 2009. TU4RAI01.
- [3] J. Jacob, Radio frequency solid state amplifiers, in: Proc. of CAS-CERN Accel. School Power Converters, Baden, Switzerland, 2015, pp. 197–216, <https://doi.org/10.5170/CERN-2015-003.197>.
- [4] J.-M. Godefroy, J. Polian, F. Ribeiro, T. Ruan, MOSFET RF power amplifier for accelerator applications, in: Proc. of 6th European Particle Accel. Conf. (EPAC 98), Stockholm, Sweden, 1998 pp.e-proc. 1811.
- [5] P. Marchand, T. Ruan, F. Ribeiro, R. Lopes, High power 352-MHz solid state amplifiers developed at the synchrotron SOLEIL, Phys. Rev. ST Accel. Beams 10 (2007) 112001.
- [6] P. Marchand, Review and prospects of RF solid state power amplifiers for particle accelerators, in: Proc. of IPAC17, Copenhagen, Denmark, 2017, pp. 2537–2542.
- [7] J. Jacob, High power RF solid state amplifiers for accelerators and storage rings, in: 60th ICFA Advanced Beam Dynamics Workshop on Future Light Sources (FLS2018), Shanghai, China, 2018.
- [8] P. Mendez, et al., LIPAc RF power system: design and main practical implementation issues, Fusion Eng Des 165 (2021) 112226, <https://doi.org/10.1016/j.fusengdes.2021.112226>.
- [9] M. Weber, D. Regidor, C. de la Morena, P. Mendez, I. Kirpitchev, J. Molla, A. Ibarra, RAMI optimization-oriented design for the LIPAC RF power system, in: Proc. of IPAC15, Richmond, VA, USA, 2015, pp. 3048–3050, <https://doi.org/10.18429/JACoW-IPAC2015-WEPMN055>.
- [10] A. Ibarra, et al., The European approach to the fusion-like neutron source: the IFMIF-DONES Project, Nucl. Fusion 59 (2019), 065002, <https://doi.org/10.1088/1741-4326/ab0d57>.
- [11] D. Regidor, et al., IFMIF-DONES RF System, Fusion Eng Des 165 (2021) 112322.
- [12] C. de la Morena, et al., Single-step port-reconfigurable cavity combiner with high efficiency, Nucl. Instrum. Methods Phys. Res. A 972 (2020), 164108, <https://doi.org/10.1016/j.nima.2020.164108>.
- [13] J. Jacob, J.-M. Mercier, M. Langlois, G. Gautier, 352.2 MHz-150 kW solid state amplifiers at the ESRF, in: Proc. of IPAC11, San Sebastián, Spain, 2011, pp. 71–73.
- [14] E. Montesinos, CERN LIU-SPS 200MHz RF upgrade: SSPA amplifiers, CWRF 2016, 2016. Grenoble, France.
- [15] D. Horan, RF developments at the advanced photon source: 352-MHz solid State RF and klystron tuning, in: 10th Continuous Wave and High Average Power RF Workshop (CWRF2018), Hsinchu, Taiwan, 2018.
- [16] T. Inagaki, H. Maesaka, T. Ohshima, T. Asaka, C. Kondo, Y. Ohashi, S. Sasaki, Upgrade status of the RF system for SPRING-8 storage ring, in: 10th Continuous Wave and high Average Power RF Workshop (CWRF2018), Hsinchu, Taiwan, 2018.
- [17] M. Gaudreau, D. Cope, E. Johnson, M. Kempkes, R. Simpson, N. Stuart, High efficiency high power resonant cavity amplifier for PIP-II, in: Proc. IPAC19, Melbourne, Australia, 2019, <https://doi.org/10.18429/JACoW-IPAC2019-THPTS095>.
- [18] F. Pérez, et al., High power cavity combiner for RF amplifiers, in: Proc. of EPAC 2006, Edinburgh, Scotland, 2006, pp. 3215–3217. THPCH179.
- [19] D. Regidor, et al., IFMIF-EVEDA RF power system, in: Proc. of IPAC11, San Sebastián, Spain, 2011, pp. 394–396. <https://accelconf.web.cern.ch/IPAC2011/papers/mopc135.pdf>.
- [20] C. de la Morena, et al., Fully digital and white rabbit-synchronized low-level RF system for LIPAC, IEEE Trans. Nucl. Sci. 65 (1) (2018) 514–522, <https://doi.org/10.1109/TNS.2017.2780906>.